ELSEVIER

Biophysical Chemistry 51 (1994) 337–347

Biophysical Chemistry

Antigen–antibody recognition. Model calculations

Vladimir V. Nauchitel [a,*], Rajmund L. Somorjai [b]

[a] *Oklahoma University Health Sciences Center, Post Office Box 26901, CHB, Rm. 115, Oklahoma City, Oklahoma 73190, USA*
[b] *Institute for Biodiagnostics, National Research Council of Canada, 435 Ellice Ave., Winnipeg, Manitoba R3B 1Y6, Canada*

Received 25 January 1994; accepted 15 February 1994

Abstract

Free energy of antigen–antibody binding has been calculated for HyHEL-5, HyHEL-10, and D1.3 complexes. We also have calculated free energies of binding per residue of L- and H- chains of the antibodies, and those of the antigen (lysozyme). The results of the calculations provide support for the notion that TYR and TRP residues may confer on the CDRs of antibodies an enhanced capacity for binding antigens. It was shown also that the composition of residues that provide major part of the binding free energy differs for antibodies and antigens.

Key words: Antigen; Antibody; Recognition; Proteins; Residues; Accessibility; Hydrophobicity

1. Introduction

The problem of antigen–antibody complex formation interweaves the problem of the influence of water with the problem of the interaction specificity. Antigen and antibody molecules form complexes in a surrounding where water is one of the essential components. There is a hypothesis about the possible importance for binding of particular residues (TYR, TRP) that are found to be present in greater than expected quantities at protein surface at the CDR areas of antibodies [1,2]. Views differ on what the essential interactions are that make the molecules form complexes. There is probably not a great difference between the nature of forces that make proteins fold and ones making proteins adhere to each other. Chothia and Janin [3] suggest that hydrophobicity is the major factor stabilizing protein–protein association, while complementarity plays a selective role in deciding which proteins may associate. These authors stress: "...while van der Waals and polar interactions contribute little to the stability of the complex, they decide which proteins may recognize each other." We share and support this view on the role of different types of interactions, but we think that the notion of hydrophobicity and electrostatic interaction needs to be related more specifically to particular residues to provide a better understanding of the roles of different residues in specific interactions of protein molecules. Here we analyze the interactions between antigens and antibodies in terms of the Gaussian neighborhood approach introduced in ref. [4] and developed in ref. [5], in order to provide a possibility of

* Corresponding author.

SSDI 0301-4622(94)00054-N

assessing free energy changes of amino acid residues on conformational changes and complex formation.

We deal with three antigen–antibody complexes: IG-G1 Fab fragment (Hy-HEL-5) and Lysozyme (E.C.3.2.1.17), IG-G1 Fab fragment (Hy-HEL-10) and Lysozyme (E.C.3.2.1.17), and IG-G1 Fab fragment (D1.3, Kappa) and Lysozyme (E.C.3.2.1.17). The X-ray structures of the complexes are described in [6–8]. To perform the calculations, coordinates of atoms were taken from the files (2hfl, 3hfm, 1fdl) of Protein Data Bank [9].

2. Probability density functions of twenty standard residues for occupying different locations in proteins, and related free energies

To study how different residues participate in antigen–antibody recognition an approach is needed that would account for the residues' surroundings in terms of free energy. Previous work [5] provides our basis for assessing free energy differences between different conformations as well as free energy of complex formation. In that study histograms that characterize propensity to occupy different locations (extent of being buried/exposed) for twenty standard amino acid residues in 64 water soluble protein molecules were calculated. Here we use the data to calculate probability density functions that allow an analytical presentation of the free energy dependence on the extent of being buried for the residues. We approximate the probability functions for every residue by the sum of two Gaussian functions

$$\rho(g_i) = \left[k_{1i}/\left(2\pi\sigma_{1i}^2\right)^{1/2}\right] \times \exp\left[-(g_i - g_{1i})^2/2\sigma_{1i}^2\right] + \left[(1-k_{1i})/\left(2\pi\sigma_{2i}^2\right)^{1/2}\right] \times \exp\left[-(g_i - g_{2i})^2/2\sigma_{2i}^2\right], \quad (1)$$

where $\rho(g_i)$ is scaled probability $\int_{-\infty}^{\infty}\rho(g)\,dg = 1$ of the Gaussian neighborhood of residue i to have value g_i which characterizes its surrounding

Table 1
Most probable, $g_{m.p.}$, average, $\langle g\rangle$, and parameters of probability density functions for amino acid residues [a]

		$g_{m.p.}$	$\langle g\rangle$	σ	g_{01}	σ_1	g_{02}	σ_2	k_1
1 PHE	(F)	52.75	48.1	6.2	47.73	5.40	53.02	1.53	0.780
2 MET	(M)	52.63	47.9	7.2	43.39	7.21	52.82	2.62	0.493
3 HIS	(H)	52.56	44.0	8.5	40.63	7.83	52.84	2.42	0.721
4 ILE	(I)	52.40	48.5	6.6	45.95	6.55	52.70	2.57	0.549
5 VAL	(V)	51.52	47.7	6.9	43.49	7.08	51.89	3.23	0.473
6 CYS	(C)	51.41	49.2	5.8	43.43	6.59	51.70	3.79	0.284
7 ALA	(A)	51.23	43.1	9.1	39.25	8.53	52 36	3.94	0.711
8 LEU	(L)	51.21	47.7	6.4	45.10	6.30	51.81	3.11	0.563
9 TRP	(W)	49.74	48.7	5.5	37.09	4.11	49.75	4.35	0.086
10 TYR	(Y)	49.56	45.9	6.4	43.06	5.88	50.60	3.36	0.601
11 ARG	(K)	39.43	39.2	7.5	39.28	8.08	39.50	2.72	0.923
12 THR	(T)	38.29	41.2	8.4	38.28	6.12	52.60	3.18	0.776
13 ASN	(N)	35.94	39.3	8.5	35.07	6.61	48.23	5.53	0.673
14 GLN	(Q)	35.83	39.7	8.0	35.48	5.88	48.34	4.73	0.674
15 GLU	(E)	35.72	38.3	7.5	35.28	5.93	47.06	4.81	0.751
16 PRO	(P)	35.50	38.9	8.1	35.07	6.35	47.93	4.91	0.717
17 ASP	(D)	35.21	38.8	8.5	34.97	6.07	49.61	5.64	0.736
18 GLY	(G)	34.76	41.0	10.1	34.55	7.56	51.64	5.39	0.624
19 LYS	(K)	34.04	34.9	6.2	33.85	4.80	37.32	8.92	0.724
20 SER	(S)	33.99	39.2	9.5	33.91	6.49	50.22	4.93	0.681

[a] σ is the dispersion of the whole distribution; g_{01}, g_{02} are positions of the two Gaussian functions, σ_1, σ_2 are their dispersions, k_1 is weight of the first Gaussian.

(or accessibility to water), see ref. [4]. (This Gaussian neighborhood is not to be confused with the two Gaussian functions used for approximation of its probability.), g_{1i}, g_{2i} are average values (or locations) of the two Gaussian functions we use for the approximation, σ_{1i}, σ_{2i} are their dispersions, $k_{1i} \leqslant 1$ is the weight of the first Gaussian function, while $(1 - k_{1i})$ is the weight of the second one. We have chosen the two Gaussian presentation for the probability profiles because the histograms [5] have two very distinctive points of clustering: residues that avoid contacts with water are grouped around one of the points while those that prefer contacts with water are grouped around the other, and almost all the profiles are asymmetrical. This asymmetry depends on the contribution of polar and nonpolar parts of each residue. The five parameters above (k_{1i}, g_{1i}, g_{2i}, σ_{1i}, σ_{2i}) have to be determined for each of the twenty standard residues. To determine the parameters we minimized sums of deviations of $\sum_{m=1}^{N}(\int_{g(m)}^{g(m+1)} g\,dg - n_m)^2$ over all histograms for each residue; n_m is probability to have a g value between $g(m)$ and $g(m+1)$. The n_m were calculated for the twenty residues from a set of 64 water soluble proteins in ref. [5].

The parameters: average values, $\langle g \rangle$, most probable values, $g_{\mathrm{m.p.}}$, as well as dispersions, σ, of the distributions for the twenty residues, are presented in Table 1. The residues in the table are divided into two groups where they are ordered according to their $g_{\mathrm{m.p.}}$ values. The composition of the groups does not depend on which of the two parameters ($g_{\mathrm{m.p.}}$, $\langle g \rangle$) of their distributions is used. It is interesting to note that the residue order in the groups depends on the parameter chosen. One group includes residues that tend to be exposed to the solvent (smaller $g_{\mathrm{m.p.}}$ or $\langle g \rangle$), while the other one includes the residues that prefer to be buried. It is easy to divide the residues into two groups because there is a very broad gap between the groups. The maximum difference between $g_{\mathrm{m.p.}}$ values in the first group does not exceed 3.2, and the maximum for the second group is less than 5.5, while the gap between the groups exceeds 10.

TRP and TYR residues occupy the two lowest positions in the group of hydrophobic residues when they are ordered according to their $g_{\mathrm{m.p.}}$ values. However, TRP would be in the second highest position after CYS if the residues were ordered according to their average values, $\langle g \rangle$, and TYR would stay near the bottom above ALA and HIS. This dependence on the chosen parameter reflects the general problem of classification of amino acid residues. Thus some papers put TRP as the most hydrophobic residue, whereas others characterize it as being less so, see for example [5,10]. The marginal positions of TRP and TYR (Table 1) may characterize their higher propensity to occupy surface locations. The fact that these residues margin the group can be attributed to the polar groups (–OH in TYR and –NH in TRP) attached to their 'rings' which should allow them to be at least partially exposed to water and thus increase their propensity to occupy surface locations. It is not that evident why ARG occupies the highest position in the second group. A possibility is that the geometry of the guanidinum part of ARG's side chain may not fit well into aqueous surroundings, perhaps because of the close distance between the $-NH_2$ groups that does not allow different water molecules to approach all of them equally well. (The environment and binding patterns of ionizable groups were analyzed in ref. [11].) The high position of THR in the hydrophilic group is due to its $-CH_3$ group, which brings this residue closer to the hydrophobic residues in comparison to other polar residues whose side chains terminate in one or two uncompromised polar groups.

Table 1 presents parameters of the function (1) for the twenty amino acid residues obtained by fitting as described above. Analysis of the parameters reveals some interesting features about the nature of the residues.

Dispersions, σ_{01}, of the first component of the distributions are wider than those, σ_{02}, of the second component for all, but TRP, in the first group. TRP's g-distribution is more symmetrical than others in this group (it has the lowest weight of the first component, $k_1 = 0.086$).

The first components of the second group residues are also broader (they have greater dispersions) than their second components for all residues, but LYS. ARG has the most symmetri-

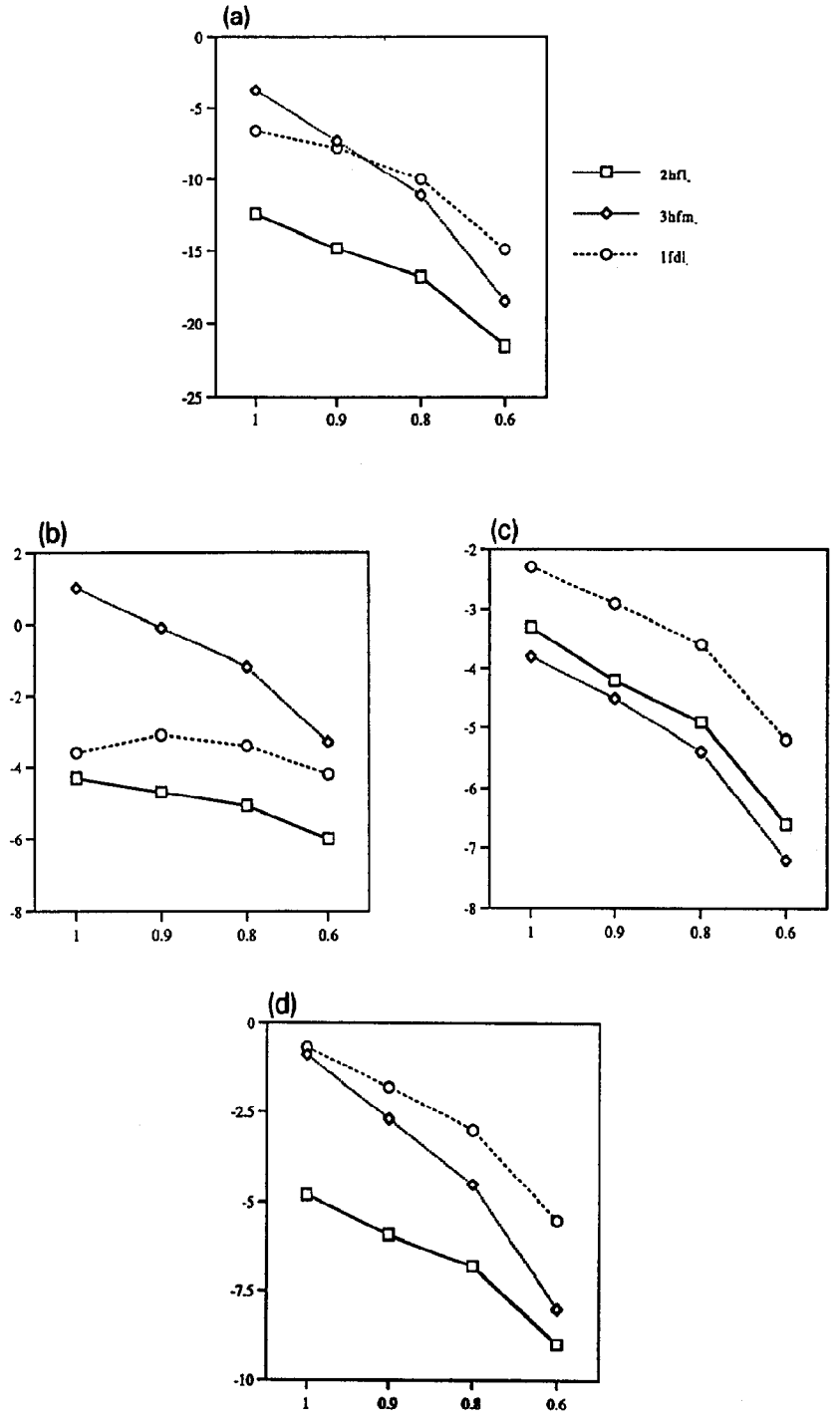

Fig. 1. Free energy of binding dependence on N for HyHEL-5, HyHEL-10, and D1.3 antigen–antibody complexes. (a) Total free energy of binding. (b) free energy of L-chains. (c) Free energy of H-chains. (d) Free energy of lysozyme.

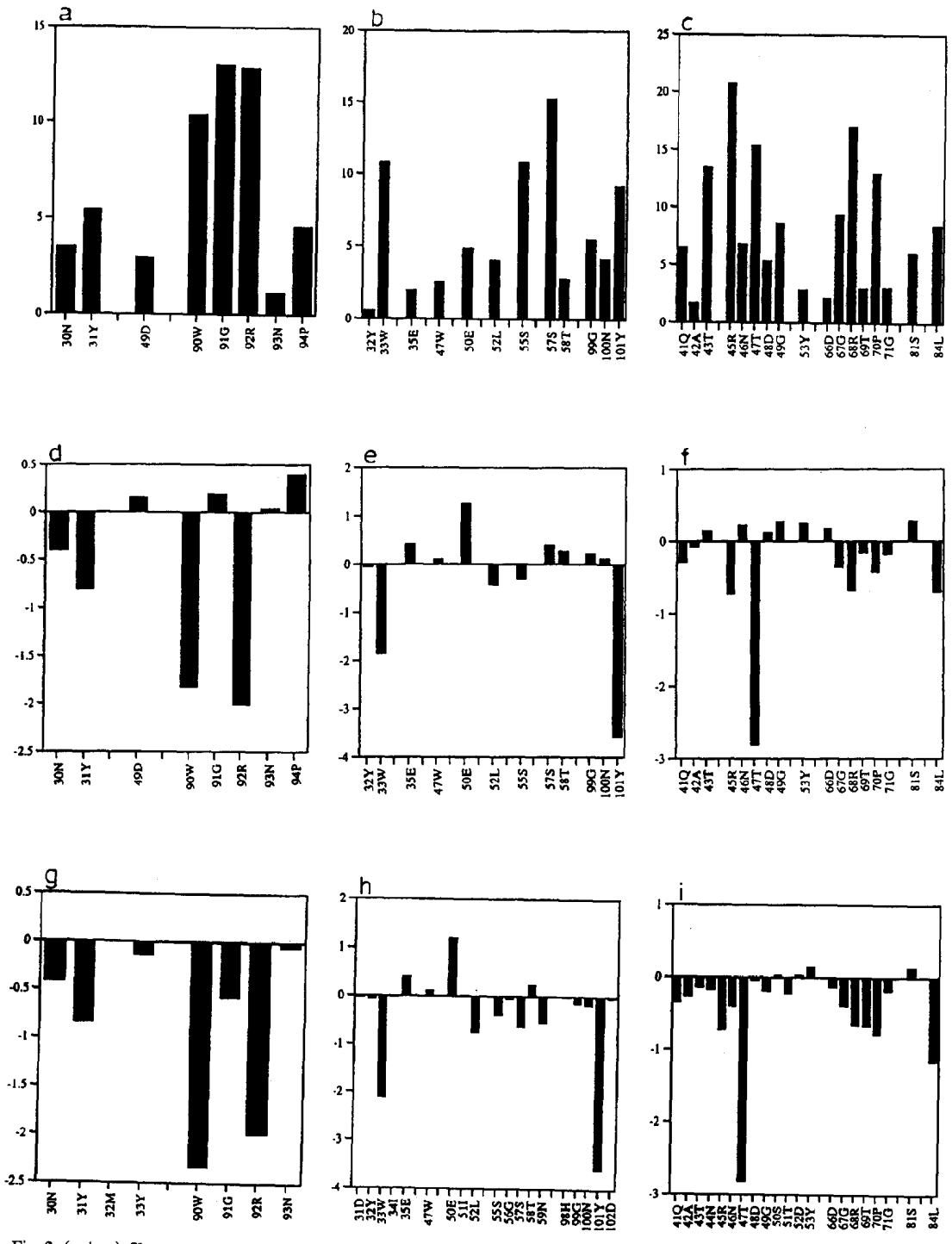

Fig. 2. (a, b, c) Change of accessibility, g, for the residues of L-, H- chains, and lysozyme caused by antigen–antibody binding, complex HyHEL-5 (2hfl file of Protein Data Bank). (d, e, f) Free energy of binding per residue of L-, H- chains, and lysozyme at $N = 1$. (g, h, i) Free energy of binding per residue of L-, H- chains, and lysozyme at $N = 0.6$.

cal g-distribution among all the residues. The distribution for ARG is characterized by almost equivalent positions of its two components (g_{01} = 39.3, g_{02} = 39.5) on one hand, and by the higher weight of its first component (k_{01} = 0.923). LYS has a wider second component, but a higher weight of the first one, k_1 = 0.724. The positions of the two components are close enough (σ_{01} = 33.8, σ_{02} = 37.3) to shape this distribution mainly around the location of the first component.

The first component of the g-distribution for an amino acid residue can be interpreted as a representation of polar or charged part of its whole distribution, while the second component can be interpreted as a representation of the nonpolar part of the residue. Then, the wider first component for the most of the residues shows that the polar component does not discriminate between inner core and outer shell as distinctly as the nonpolar does.

Analytical presentation of the probability distribution functions allows one to estimate free energy change for each residue whose exposure to solvent changes on conformational change or binding. The relation between the free energy and the probability distribution is defined by

$$\exp\{[F(g) - F(g_{\mathrm{m.p.}})]/RT\} = \rho(g_{\mathrm{m.p.}})/\rho(g). \quad (2)$$

Thus the relative free energy of a residue is

$$[F(g) - F(g_{\mathrm{m.p.}})]/RT = \ln[\rho(g_{\mathrm{m.p.}})/\rho(g)]. \quad (3)$$

We do not know absolute values of $F(g)$ and $F(g_{\mathrm{m.p.}})$ but we can estimate $\Delta F = F(g) - F(g_{\mathrm{m.p.}})$ for every residue at different surroundings which are characterized by their g values. We use the letter F here for Gibbs free energy to avoid confusion with Gaussian neighborhood. Eq. (1) and the data of Table 1 are used to calculate the probability density $\rho(g)$ and $\rho(g_{\mathrm{m.p.}})$ that are needed for Eq. (3).

Physico-chemical conditions (temperature, ionic strength, pH, etc.) can change the energetics of protein molecules in a solvent. Thus it was shown that the stability of the globular state of a protein may depend strongly on pH [12]. In our model the influence of the physico-chemical conditions in a solvent may be interpreted in terms of residue propensity to be exposed or buried, which should depend on the conditions. The two Gaussian distribution (1) allows to vary the ratio between the hydrophobic and hydrophilic components in our model. In order to control the ratio we introduced one more parameter, N, which changes k_1 in Eq. (1) to $k_1^* = k_1\mathrm{N}$ and k_2 to $k_2^* = 1 - k_1^*$, $(0 \leqslant \mathrm{N} \leqslant 1)$.

3. Free energy of complex formation

In this paper we assess free energy of binding as the difference between the sum of free energies of all the residues for complexed molecules and the sums for lysozyme and the antibodies separately. We use the same structures of single molecules (lysozyme and antibodies) as those in the appropriate complexes. Formation of the complexes leads to additional shielding of some of the residues of the antibodies and antigens. Relation between the residue exposure and free energy is expressed by Eqs. (1), (2) and (3). The sum over all the residues gives an estimate of that part of free energy of binding that does not account for conformational changes of the molecules at the preliminary stage of the complex formation, and thus is not exactly the whole binding energy. The additional screening of residues reveals itself through their increased g values that come from the molecules' complex formation. Actually, we calculated sums of $\ln[\rho(g_{\mathrm{m.p.}})/\rho(g)]$ over all the residues of L- (light) and H- (heavy) chains of antibody and over residues of lysozyme molecule for each of the three complexes. Free energy change in our case is an additive sum over all residues whose g values (G-neighborhood) change on binding.

The dependence of calculated free energy of binding on parameter N for the three antigen–antibody complexes is shown in Figs. 1a–d. The initial value N = 1 brings low binding energies in comparison to experimental ones ($\Delta F/RT$ at 300 K ranges for HyHEL-5 from −21.6 to −23.4; HyHEL-10, −21.1 to −22.1; and D1.3, −17.6 to −18.7 [7,13]) and places D1.3 and HyHEL-10 in

a wrong order, while lower values of N deliver the correct order for all three complexes and the energies get close to the experimental values at N = 0.6, Fig. 1a. We have also calculated the free energy of binding for L- and H-chains of the antibodies, Figs. 1b and 1c, and the free energy

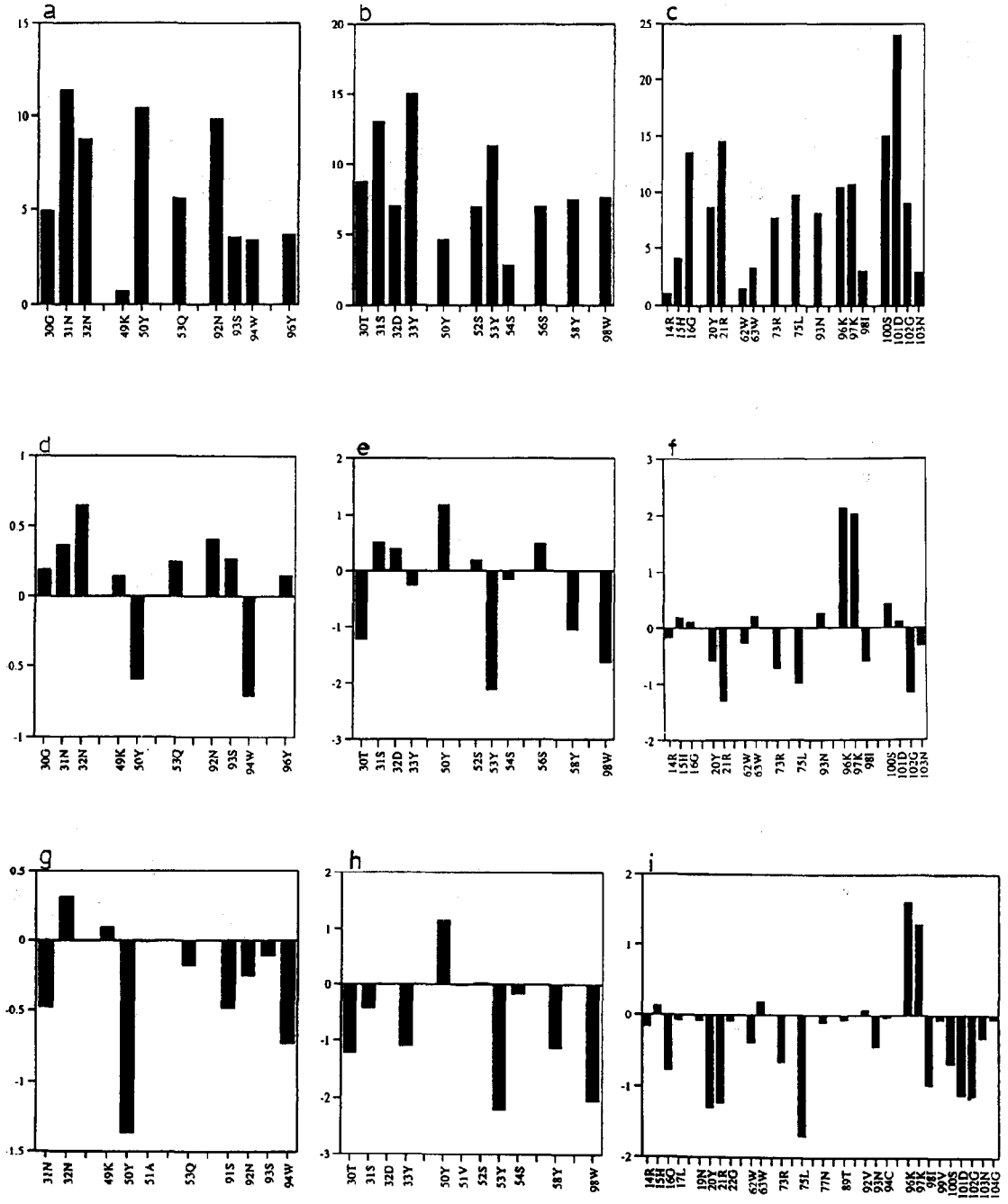

Fig. 3. Same as Fig. 2 for HyHEL-10 (3hfm file).

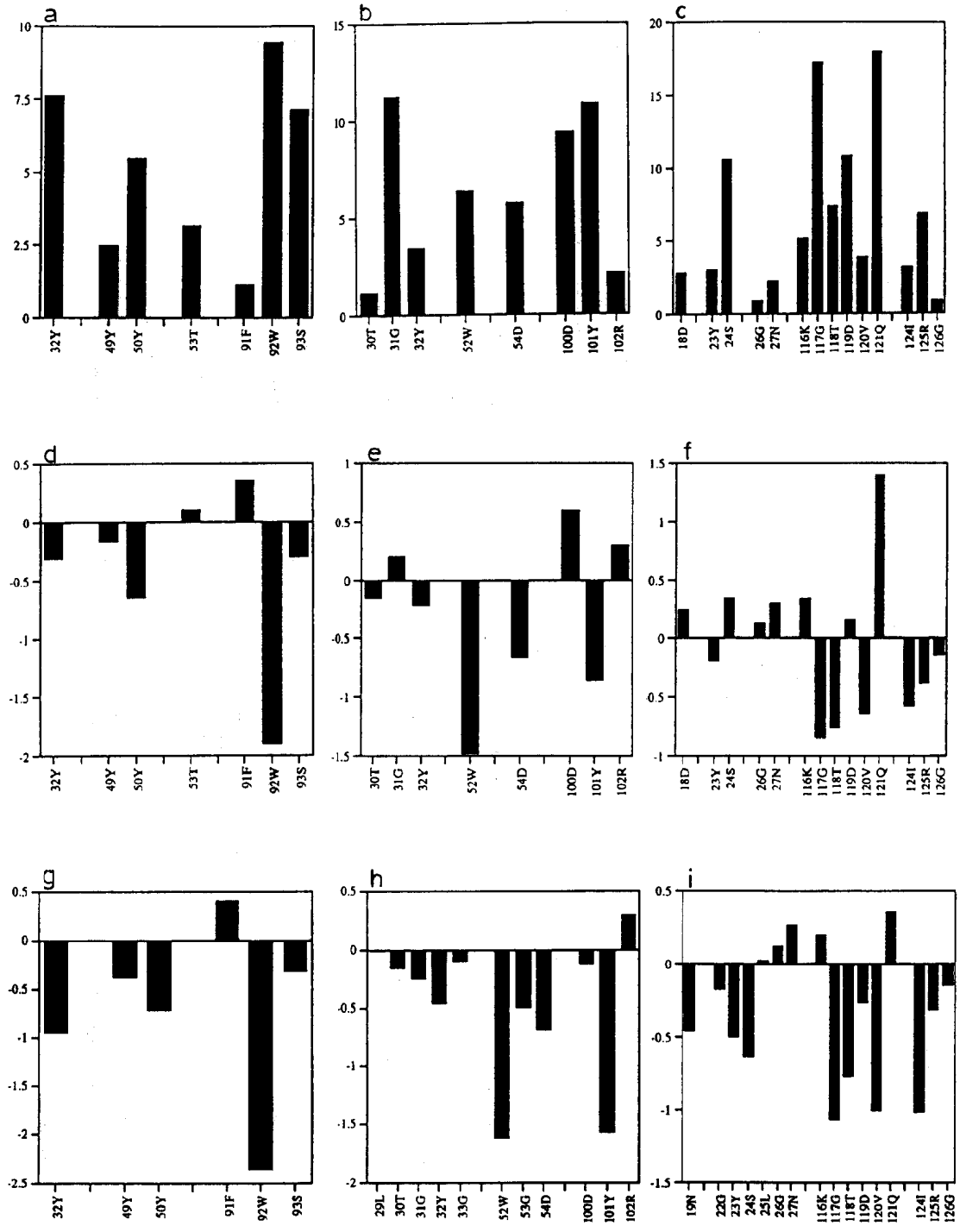

Fig. 4. Same as Fig. 2 for D1.3 (1fdl file).

for lysozyme, Fig. 1d. The binding free energies of L- and H-chains do not quite follow these for the complexes; L-chain of D1.3 interacts stronger with the antigen than L-chain of HyHEL-10, while the interaction of H-chain of HyHEL-10 is the strongest among the three. The binding energies of the antigen mainly follow the order of the experimental results for the complexes.

The change of accessibility per residue as well as the free energy of binding per residue for the three complexes are presented in Figs. 2, 3 and 4. Figs. 2a–2c, 3a–3c and 4a–4c show how the g values change on the antigen–antibody binding for L-chain, H-chain and lysozyme residues, thus revealing which residues participate in the intermolecular contacts and how big their involvement is. Figs. 2d–2f, 3d–f and 4d–4f show free energy change for each residue participating in binding at $N = 1$, and Figs. 2g–2i, 3g–3i and 4g–4i show the energies at $N = 0.6$. The free energy of antigen–antibody binding is sum of these residues' free energy changes.

There are TYR and TRP residues on the contacting surfaces of all three antibodies. These residues provide the main part of the free energy that stabilizes the complexes, see Figs. 2,3 and 4 (d through i). The pattern of the antigen's residues participating in contact with antibodies and stabilizing the complexes differs from that one of antibodies. Thus GLN(41), ARG(45), THR(47), GLY(67), ARG(68), THR(69), PRO(70), LEU(84) residues of lysozyme stabilize HyHEL-5 complex, TYR(23), GLY(117), THR(118), VAL(120), ILE(124), ARG(125) and GLY(126) of lysozyme provide stabilizing effect in D1.3 complex, and ARG(14), TYR(20), ARG(21), TRP(62), ARG(73), LEU(75), ILE(98), GLY(102) and ASN(103) of lysozyme stabilize HyHEL-10 complex. First of all, the antibodies and antigens differ in the composition of residues that participate in stabilizing the complexes. There is only one residue with nonpolar aliphatic side chain (LEU(52H), of HyHEL-5 complex; 52H stands for residue 52 of H-chain) among all the contacting residues of the three antibodies, whereas the antigen epitopes of all three complexes have such contacting residues (LEU(84) of HyHEL-5; VAL(120) and ILE(124) of D1.3; LEU(75) and ILE(98) of HyHEL-10). Another common stabilizing residue of the antigens is ARG (ARG(45), ARG(68) of HyHEL-5; ARG(125) of D1.3; ARG(21), ARG(73) of HyHEL-10). The plots (d,e,f) and (g,h,i) of Figs. 2–4 show that the contribution of participating in binding residues depends on N while the pattern of their main stabilizing and destabilizing residues remains practically unchanged for the two N values.

As we pointed out before, TRP and TYR margin the group of hydrophobic residues, whereas as THR and ARG margin the group of hydrophilic residues. These pairs of residues belong to the two different groups, but have $g_{\text{m.p.}}$ values that are the closest among all the residues of the two groups, see Table 1. Their marginal positions in their groups characterize their higher probability to occupy locations in proteins that are more appropriate for the residues of the opposite group. And this means, if they really occupy such locations, they are more inclined to give them up if a suitable situation occurs, as in case of when an antibody meets its antigen. We think that these four residues are crucial for specific recognition by antibodies. Other polar and charged residues also help to form specific complexes through preventing nonspecific complex formation where lost electrostatic interaction with water cannot be compensated through 'lock-key' (optimal) interaction between positive and negative charges.

4. Conclusion

It is interesting to compare our results with those obtained with a more explicit approach to dealing with different types of interactions. There are two common complexes (D1.3 and HyHEL-5) in this work and in the work [14] where a more explicit approach is used. The authors assume that no conformational changes occur upon complex formation, so they deal with 'rigid body' model, the simplest possible concept of noncovalent complex formation. The free energies of binding ($\Delta F/RT$) from their work are -15.0 ± 5 for D1.3 complex and -53.3 ± 8.3 for HyHEL-5 (we converted their values into dimensionless free

energies for $T = 300$ K). The value for D1.3 is close to the experimental one (−17.6 through −18.7), whereas the value for HyHEL-5 is too big to be good (experiments give values −21.6 through −23.6 [7,13]). The authors discuss possible sources of this disagreement. The simplification of the 'rigid body' approach is common for the cited paper and ours. Our results on the binding energies of different antibody residues for D1.3 and HyHEL-5 antigen–antibody complexes differ from those in ref. [14]. In case of D1.3, L-chain, our approach shows the largest binding energy for TRP 92, next follows TYR 32 and TYR 50 and almost nothing for HIS 30, Fig. 4, whereas, in [14] the order is as follows TYR 50, HIS 30, TRP 92 and no data on TYR 32. For H-chain of D1.3 we have the following order of residues TRP 52, TYR 101, ASP 54, TYR 32 (the first residue having the largest binding energy and the last one the smallest energy), while the order in above paper is ASP 100, GLY 31, TYR 101, ARG 99, TRP 52. Our data for L-chain of antibody in HyHEL-5 complex put the binding residues in order TRP 90, ARG 92, TYR 31, GLY 91, ASN 30, which is close to that of ref.] [14], with the order ARG 92, TRP 90, GLY 91, TYR 31, but our data for H-chain of the complex (TYR 101, TRP 33, LEU 52, SER 57, Fig. 2) differ strongly from their results (GLU 50, GLU 35, TRP 33, ASN 59, TYR 101). Our approach gives positive values for binding free energies of GLU 50 and GLU 35, which means that they destabilize the complex, whereas their having H-bonds or forming salt bridges with residues of the antigen stabilize the complex's structure. It is possible that H-bonding and salt bridging will destabilize the complexes energetically while stabilizing them structurally. There are other interactions than H-bonds and salt bridges that stabilize the complexes, whereas the transfer of these charged residues from water surrounding, where they strongly interact with water molecules, into the antigen–antibody interface where they form new salt bridges and/or H-bonds influences the mutual orientation of the complex molecules, but may not provide for the complete compensation of the free energy. It may look as if the approach [14], that deals with some of the interactions explicitly, is advantageous to ours, but its main problem of how to treat electrostatic interactions of charged and polar groups correctly to account for the transfer between water and the complex interface is a weak point of similar approaches, as noted by the authors. On the other hand, strong stabilizing involvement of TYR and TRP residues in binding (large negative free energies) delivered by our approach correlates well with the fact that both chains (L- and H-) of all the CDRs have these residues. These residues are present and stand out among the CDR residues of all three antibodies, but not among the residues of the antigenic determinants.

An unusual residue composition for the surface of proteins (the presence of TYR and TRP residues) was stressed for the CDR parts of antibodies in ref. [1]. The author thinks that these unusual structural features may confer on these sites an enhanced capacity for binding ligands and thus make them especially suited for interacting with ligands. Our results provide support for this view. Our approach identifies TYR and TRP residues as providing energetically largest portions of the antibodies' binding free energies, although there is one exception, ARG92 in L-chain of complex HyHEL-5. Even though our approach uses the free energies that are average values over different surroundings (free energy profiles) and, therefore cannot provide an absolute assessment for particular local situations, the result of picking up these two residues which are present in all the three antibodies suggests its ability to discriminate residues that are responsible for the specificity of different antibodies.

References

[1] E.A. Padlan, Prot. Struct. Funct. Gen. 7 (1990) 112–124.
[2] I.S. Mian, A.R. Bradwell and A.J. Olson, J. Mol. Biol. 217 (1991) 133–151.
[3] C. Chothia and J. Janin, Nature 256 (1975) 705–708.
[4] V.V. Nauchitel and R.L. Somorjai, Prot. Struct. Funct. Gen. 15 (1993) 50–61.
[5] V.V. Nauchitel and R.L. Somorjai, Biophys. Chem. 51 (1994) 327.
[6] A.G. Amit, R.A. Mariuzza, S.E.V. Phillips and R.J. Poljak, Science 233 (1986) 747–753.
[7] E.A. Padlan, E.W. Silverton, S. Sheriff, G.H. Cohen, S.J.

Smith-Gill and D.R. Davies, Proc. Natl. Acad. Sci. USA 86 (1989) 5938–5942.

[8] S. Silverton, E.W. Sheriff, E.A. Padlan, G.H. Cohen, S.J. Smith-Gill, B.C. Finzel and D.R. Davies, Proc. Natl. Acad. Sci. USA 84 (1987) 8075–8079.

[9] E.E. Abola, F.C. Bernstein, S.H. Bryant, T.F. Koetzle and J. Weng, Protein Data Bank in Crystallographic Databases-Information Content, Software Systems, Scientific Applications, eds. F.H. Allen, G. Bergerhoff and R. Sievers (Data Commission of the International Union of Crystallography, Bonn/Cambridge/Chester, 1987) pp. 107–132.

[10] J.L. Cornette, K.B. Cease, H. Margalit, J.L. Spouge, J.A. Berzofsky and C. DeLisi, J. Mol. Biol. 195 (1987) 659–685.

[11] A.A. Rashin and B. Honig, J. Mol. Biol. 173 (1984) 515–521.

[12] P.L. Privalov, Yu.V. Grico, S.Yu. Venyaminov and V.P. Kutyshenko, J. Mol. Biol. 190 (1986) 487–498.

[13] M. Harper, F. Lema, G. Boulot and R.J. Poljak, Mol. Immunol. 24 (1987) 97–108.

[14] J. Novotny, R.E. Bruccoleri and F.A. Saul, Biochemistry 28 (1989) 4735–4748.